Substituent Effects in Pentacenes: Gaining Control over HOMO–LUMO Gaps and Photooxidative Resistances

ARTICLE *in* JOURNAL OF THE AMERICAN CHEMICAL SOCIETY · DECEMBER 2008

Impact Factor: 12.11 · DOI: 10.1021/ja804515y · Source: PubMed

8 AUTHORS, INCLUDING:

Mehmet R Dokmeci
Brigham and Women's Hospital
164 PUBLICATIONS **2,364** CITATIONS
SEE PROFILE

Chandrani Pramanik
University of Colorado Boulder
11 PUBLICATIONS **166** CITATIONS
SEE PROFILE

Nicol Mcgruer
Northeastern University
106 PUBLICATIONS **1,904** CITATIONS
SEE PROFILE

Article

Substituent Effects in Pentacenes: Gaining Control over HOMO#LUMO Gaps and Photooxidative Resistances

Irvinder Kaur, Wenling Jia, Ryan P. Kopreski, Selvapraba Selvarasah, Mehmet R. Dokmeci, Chandrani Pramanik, Nicol E. McGruer, and Glen P. Miller

J. Am. Chem. Soc., **2008**, 130 (48), 16274-16286 • Publication Date (Web): 12 November 2008

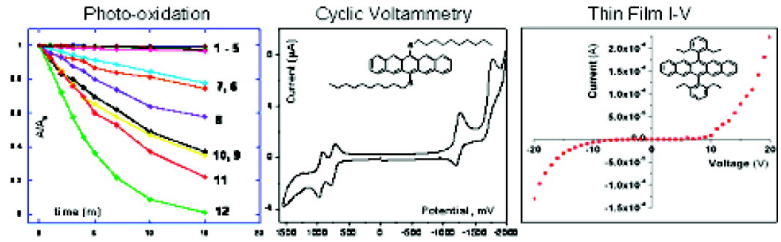

More About This Article

Additional resources and features associated with this article are available within the HTML version:

- Supporting Information
- Access to high resolution figures
- Links to articles and content related to this article
- Copyright permission to reproduce figures and/or text from this article

View the Full Text HTML

J|A|C|S
ARTICLES

Published on Web 11/12/2008

Substituent Effects in Pentacenes: Gaining Control over HOMO−LUMO Gaps and Photooxidative Resistances

Irvinder Kaur,[†] Wenling Jia,[†] Ryan P. Kopreski,[†] Selvapraba Selvarasah,[‡] Mehmet R. Dokmeci,[‡] Chandrani Pramanik,[†] Nicol E. McGruer,[‡] and Glen P. Miller*,[†]

Department of Chemistry and Materials Science Program, University of New Hampshire, Durham, New Hampshire 03824-3598, and Department of Electrical and Computer Engineering, Northeastern University, Boston, Massachusetts 02115

Received June 13, 2008; E-mail: glen.miller@unh.edu

Abstract: A combined experimental and computational study of a series of substituted pentacenes including halogenated, phenylated, silylethynylated and thiolated derivatives is presented. Experimental studies include the synthesis and characterization of six new and six known pentacene derivatives and a kinetic study of each derivative under identical photooxidative conditions. Structures, HOMO−LUMO energies and associated gaps were calculated at the B3LYP/6-311+G**//PM3 level while optical and electrochemical HOMO−LUMO gaps were measured experimentally. The combined results provide for the first time a quantitative assessment of HOMO−LUMO gaps and photooxidative resistances for a large series of pentacene derivatives as a function of substituents. The persistence of each pentacene derivative is impacted by a combination of steric resistance and electronic effects as well as the positional location of each substituent. Silylethynyl-substituted pentacenes like TIPS-pentacene possess small HOMO−LUMO gaps but are not the longest lived species under photooxidative conditions, contrary to popular perception. A pentacene derivative with both chlorine substituents in the 2,3,9,10 positions and *o*-alkylphenyl substituents in the 6,13 positions is longer lived than TIPS-pentacene. Of all the derivatives studied, alkylthio- and arylthio-substituted pentacenes are most resistant to photooxidation, possess relatively small HOMO−LUMO gaps and are highly soluble in a variety of organic solvents. These results have broad implications for the field of organic molecular electronics where OFET, OLED, and other applications can benefit from highly persistent, solution processable pentacene derivatives.

Introduction

Pentacene is one of the most widely utilized organic semiconductor compounds.[1] Due to its poor solubility and facile photodegradation,[2] numerous groups have prepared pentacene derivatives bearing either solubilizing or stabilizing substituents. Among the most commonly prepared derivatives are phenyl-substituted pentacenes[2a,3] and ethynyl-substituted pentacenes[2b,4] including silylethynyl derivatives.[3c,5] Because phenyl substituents lie in a time-averaged orthogonal orientation relative to the acene backbone, they diminish intermolecular $\pi-\pi$ stacking interactions, improve solubilities, and enable an exploration of solution-phase chemistries.[6] Phenyl-substituted pentacenes have been studied extensively as red emitters in organic light-emitting diode (OLED) applications.[3d,7]

The first silylethynyl-substituted pentacene is less than 10 years old and was prepared for the purpose of studying [60]fullerene Diels−Alder chemistry.[3c] Silylethynyl-substituted pentacenes are, however, more widely known for their electronic properties, especially as they relate to organic field-effect transistor (OFET) applications.[5b,8] The most popular of these derivatives is 6,13-bis(triisopropylsilylethynyl)pentacene or TIPS-

[†] University of New Hampshire.
[‡] Northeastern University.

(1) Chason, M.; Brazis, P. W., Jr.; Zhang, J.; Kalyanasundaram, K.; Gamota, D. R. *Proc. IEEE* **2005**, *93*, 1348–1356.
(2) (a) Ono, K.; Totani, H.; Hiei, T.; Yoshino, A.; Saito, K.; Eguchi, K.; Tomura, M.; Nishida, J.; Yamashita, Y. *Tetrahedron* **2007**, *63*, 9699–9704. (b) Palayangoda, S. S.; Mondal, R.; Shah, B. K.; Neckers, D. C. *J. Org. Chem.* **2007**, *72*, 6584–6587. (c) Etienne, A.; Beauvois, C. *Compt. Rend.* **1954**, *239*, 64–66.
(3) (a) Allen, C. F. H.; Bell, A. *J. Am. Chem. Soc.* **1942**, *64*, 1253–1260. (b) Miller, G. P.; Mack, J. *Org. Lett.* **2000**, *2*, 3979–3982. (c) Miller, G. P.; Mack, J.; Briggs, J. *Org. Lett.* **2000**, *2*, 3983–3986. (d) Jang, B.-B.; Lee, S. H.; Kafafi, Z. H. *Chem. Mater.* **2006**, *18*, 449–457. (e) Miao, Q.; Chi, X.; Xiao, S.; Zeis, R.; Lefenfeld, M.; Siegrist, T.; Steigerwald, M. L.; Nuckolls, C. *J. Am. Chem. Soc.* **2006**, *128*, 1340–1345. (f) Zhao, Y.; Mondal, R.; Neckers, D. C. *J. Org. Chem.* **2008**, *73*, 5506–5513.
(4) (a) Miller, G. P.; Mack, J.; Briggs, J. B. *Fullerenes: Proceedings of the International Symposium on Fullerenes, Nanotubes, and Carbon Nanoclusters*; Kamat, P. V., Guldi, D. M., Kadish, K. M., Eds.; The Electrochemical Soc.: Pennington, NJ, 2001; Vol. 11, pp 202−206. (b) Li, Y.; Wu, Y.; Liu, P.; Prostran, Z.; Gardner, S.; Ong, B. S. *Chem. Mater.* **2007**, *19*, 418–423.
(5) (a) Troisi, A.; Orlandi, G.; Anthony, J. E. *Chem. Mater.* **2005**, *17*, 5024–5031. (b) Anthony, J. E. *Angew. Chem., Int. Ed.* **2008**, *47*, 452–483. (c) Benard, C. P.; Geng, Z.; Heuft, M. A.; VanCrey, K.; Fallis, A. G. *J. Org. Chem.* **2007**, *72*, 7229–7236. (d) Jiang, J.; Kaafarani, B. R.; Neckers, D. C. *J. Org. Chem.* **2006**, *71*, 2155–2158. (e) Okamoto, T.; Bao, Z. *J. Am. Chem. Soc.* **2007**, *129*, 10308–10309.
(6) Briggs, J. B.; Miller, G. P. C. R. *Chimia* **2006**, *9*, 916–927.
(7) (a) Wolak, M. A.; Jang, B.-B.; Palilis, L. C.; Kafafi, Z. H. *J. Phys. Chem. B* **2004**, *108*, 5492–5499. (b) Picciolo, L. C.; Murata, H.; Kafafi, Z. H. *Appl. Phys. Lett.* **2001**, *78*, 2378–2380.

10.1021/ja804515y CCC: $40.75

pentacene.[9] The literature reveals a general acceptance that silylethynyl-substituted pentacenes like TIPS-pentacene are relatively stable species.[2b,5b,d,e] Other pentacene derivatives that have been described as stable include phenethynyl derivatives[4b] and those bearing electron-withdrawing groups like halogen, cyano, trifluoromethyl,[10] and pentafluorophenyl.[2a] Although the term stability is thermodynamic in origin, it is meant to imply a resistance to degradation or "kinetic stability" where pentacenes and other acenes are concerned. For pentacene derivatives, degradation generally involves photooxidation[2,3f] and, to a lesser extent, photodimerization.[5c,11]

Despite the large number of assertions concerning the stability of various pentacene derivatives, kinetic data to support these claims is either scarce[12] or missing altogether. Instead, a body of anecdotal evidence has emerged. For example, the widely held belief that silylethynyl-substituted pentacenes like TIPS-pentacene are among the most stable pentacene derivatives is seemingly corroborated by the fact that bulky silylethynyl substituents were successfully employed in the synthesis of persistent hexacene and heptacene derivatives,[13] a significant accomplishment. There are in fact no other reports of persistent hexacene and heptacene derivatives. Nonetheless, the absence of quantitative data to support these perceptions leaves many questions unanswered including each of the following: Do silylethynyl groups stabilize pentacene through electronic effects or steric resistance or a combination of the two? Do other substituents on pentacene also provide for enhanced photooxidative resistance? How does the positional location of substituents impact HOMO−LUMO gaps and photooxidative resistances? At what level of theory are calculated HOMO−LUMO energies and associated gaps consistent with experiment? Quantitative data that address these and related questions would help to provide a fundamental understanding of substituent effects in pentacenes, enabling the rational design of new derivatives with superior properties.

Here, we report a combined experimental and computational study of a series of substituted pentacenes including halogenated, phenylated, silylethynylated, and thiolated derivatives. Experimental studies include the synthesis and characterization of six new and six known pentacene derivatives and a kinetic study of each derivative under identical photooxidative conditions. Computationally, we calculated the structures, HOMO−LUMO energies and associated gaps at the B3LYP/6-311+G**//PM3 level for several pentacene derivatives. The calculated HOMO and LUMO energies and associated gaps complement experimental numbers obtained via UV−vis and cyclic voltammetry studies. The results provide for the first time a quantitative assessment of HOMO−LUMO gaps and photooxidative resistances for a series of pentacene derivatives as a function of substituents. Steric hindrance, electronic effects, and the positional location of substituents are key parameters for determining HOMO−LUMO gaps and photooxidative resistances. Most remarkable are alkylthio- and arylthio-substituted pentacenes. Simple to prepare[14] but little studied, alkylthio- and arylthio-substituted pentacenes possess relatively small HOMO−LUMO gaps and are considerably more resistant to photooxidation than all other pentacene derivatives tested. They also possess excellent solubility in organic solvents and therefore represent promising candidates for thin-film OFET, OLED,[15] and organic photovoltaic[16] (OPV) applications.

Results and Discussion

Synthesis and Characterization. Soluble pentacene derivatives **1**−**12** (Figure 1) were synthesized (Scheme 1), purified and then characterized by a combination of ^{1}H and ^{13}C NMR spectroscopies, UV−vis spectroscopy, high-resolution mass spectrometry (HR-MS) and cyclic voltammetry (CV). Thus, 6,13-bis(phenylthio)pentacene **1** and 6,13-bis(decylthio)pentacene **2** were prepared using the method of Kobayashi and co-workers[14] starting from pentacene-6,13-dione. TIPS-pentacene **4** was prepared using the Swager modification[17] of Anthony's synthesis.[9] All remaining pentacene derivatives were prepared using a modified Kafafi procedure.[7] Pentacene derivatives **2**, **3**, **7**, **8**, **10**, and **11** are all new compounds.

Kinetics of Photooxidation. For kinetic analyses, the purified pentacene derivatives were separately dissolved in CH_2Cl_2 to give 2.0×10^{-4} M solutions and were then exposed to ambient light and air at 25 °C for appropriate periods. UV−vis spectra were recorded at regular intervals enabling a determination of absorbance−time profiles for both the starting pentacene derivatives as well the corresponding oxidation products. Figure 2 is illustrative. Here, the long-wavelength bands of 6,13-bis(*o*-methylphenyl)pentacene, **6**, at 604, 557, and 518 nm are all observed to diminish with reaction progress while a new set of bands at 386 and 366 nm, corresponding to oxidation products, are observed to grow. Oxidation products were characterized by ^{1}H and ^{13}C NMR spectroscopy. Most pentacene derivatives did not oxidize to give a single oxidation product in a clean reaction, compounds **1**, **2**, **7**, and **12** representing exceptions. Apparent $^1O_2$ adducts **13** and **14** formed cleanly (Scheme 2) from **7** and **12**, respectively, and were subsequently isolated and characterized. Thiopentacene derivatives **1** and **2** oxidize slowly to give predominantly pentacene-6,13-dione and either diphenyl disulfide or didecyl disulfide, respectively (Scheme 3). Absorbance−time profiles (Figure 3) were determined for each pentacene derivative, and they revealed a relative ordering of photooxidative resistances as follows: 6,13-bis(phenylthio)pentacene (**1**) > 6,13-bis(decylthio)pentacene (**2**) > 2,3,9,10-tetrachloro-6,13-bis(2′,6′-dimethylphenyl)pentacene (**3**) > 6,13-TIPS-pentacene (**4**) > 6,13-bis(*o*-alkylphenyl)pentacenes (**5**, **6**) > other phenyl-substituted pentacenes (**7**−**12**).

(8) (a) Park, S. K.; Jackson, T. N.; Anthony, J. E.; Mourey, D. A. *Appl. Phys. Lett.* **2007**, *91*, 063514/1−063514/3. (b) Lee, W. H.; Kim, D. H.; Jang, Y.; Cho, J. H.; Hwang, M.; Park, Y. D.; Kim, Y. H.; Han, J. I.; Cho, K. *Appl. Phys. Lett.* **2007**, *90*, 132106/1–132106/3. (c) Park, J. G.; Vasic, R.; Brooks, J. S.; Anthony, J. E. *J. Low Temp. Phys.* **2006**, *142*, 387–392. (d) Kim, Y.-H.; Lee, Y. U.; Han, J.-I.; Han, S.-M.; Han, M.-K. *J. Electrochem. Soc.* **2007**, *154*, H995−H998. (e) Park, S. K.; Anthony, J. E.; Jackson, T. N. *IEEE Electron. Device Lett.* **2007**, *28*, 877–879.

(9) Anthony, J. E.; Brooks, J. S.; Eaton, D. L.; Parkin, S. R. *J. Am. Chem. Soc.* **2001**, *123*, 9482–9483.

(10) (a) Okamoto, T.; Senatore, M. L.; Ling, M.-M.; Mallik, A. B.; Tang, M. L.; Bao, Z. *Adv. Mater.* **2007**, *19*, 3381–3384. (b) Swartz, C. R.; Parkin, S. R.; Bullock, J. E.; Anthony, J. E.; Mayer, A. C.; Malliaras, G. G. *Org. Lett.* **2005**, *7*, 3163–3166.

(11) (a) Coppo, P.; Yeates, S. G. *Adv. Mater.* **2005**, *17*, 3001–3005. (b) Birks, J. B.; Appleyard, J. H.; Pope, R. *Photochem. Photobiol.* **1963**, *2*, 493–495.

(12) Maliakal, A.; Raghavachari, K.; Katz, H.; Chandross, E.; Siegrist, T. *Chem. Mater.* **2004**, *16*, 4980–4986.

(13) Payne, M. M.; Parkin, S. R.; Anthony, J. E. *J. Am. Chem. Soc.* **2005**, *127*, 8028–8029.

(14) Kobayashi, K.; Shimaoka, R.; Kawahata, M.; Yamanaka, M.; Yamaguchi, K. *Org. Lett.* **2006**, *8*, 2385–2388.

(15) Lee, S.; Koo, B.; Park, J.-G.; Moon, H.; Hahn, J.; Kim, J. M. *MRS Bull.* **2006**, *31*, 455–459.

(16) Rand, B. P.; Genoe, J.; Heremans, P.; Poortmans, J. *Prog. Photovoltaics* **2007**, *15*, 659–676.

(17) Kim, Y.; Whitten, J. E.; Swager, T. M. *J. Am. Chem. Soc.* **2005**, *127*, 12122–12130.

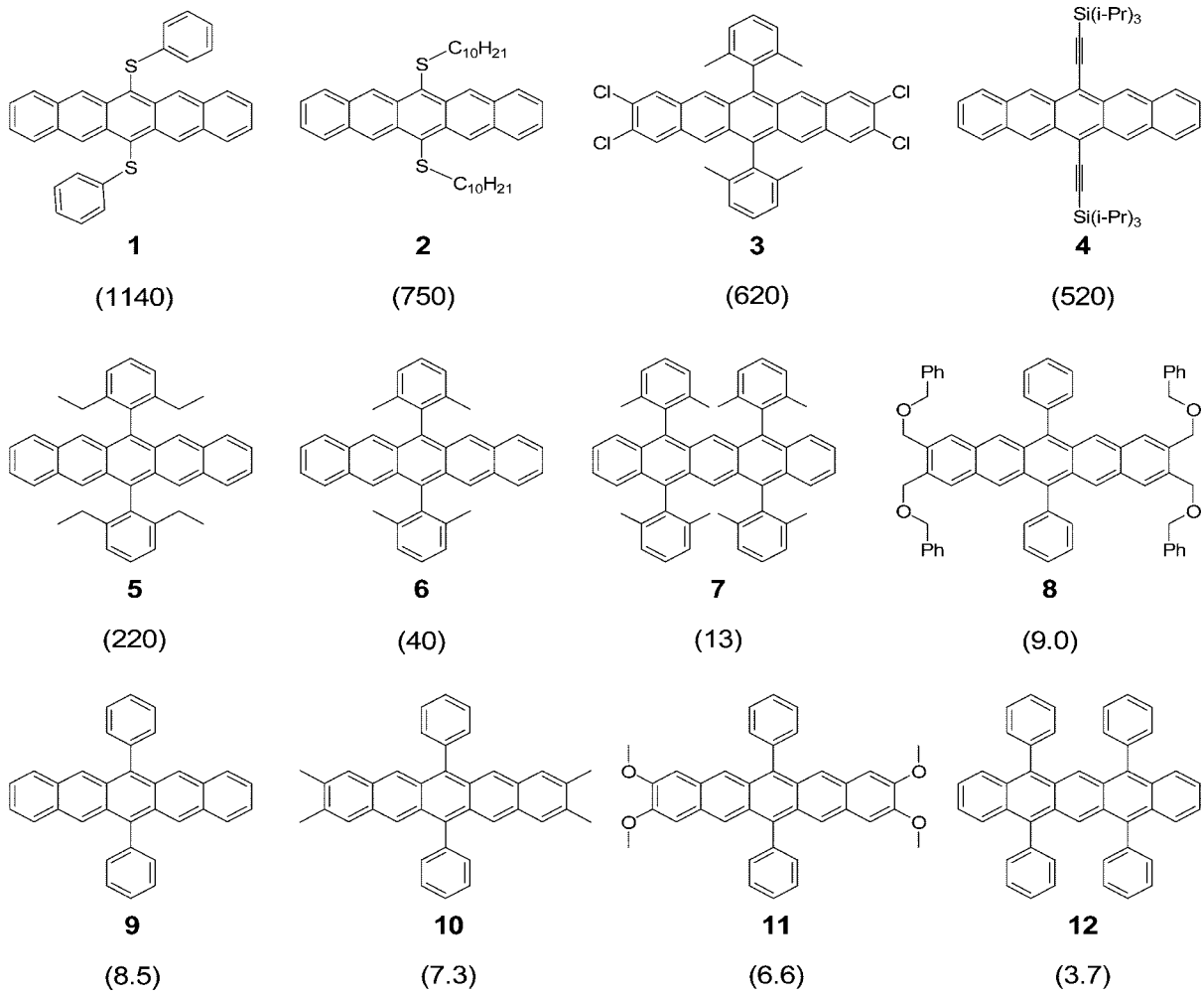

Figure 1. Structures of pentacene derivatives **1**−**12** with their associated half-lives in minutes shown in parentheses. Half-lives were determined for 2.0×10^{-4} M solutions in CH_2Cl_2 at 25 °C exposed to ambient light and air.

Scheme 1. Synthesis of Soluble Pentacene Derivatives **1**−**12**

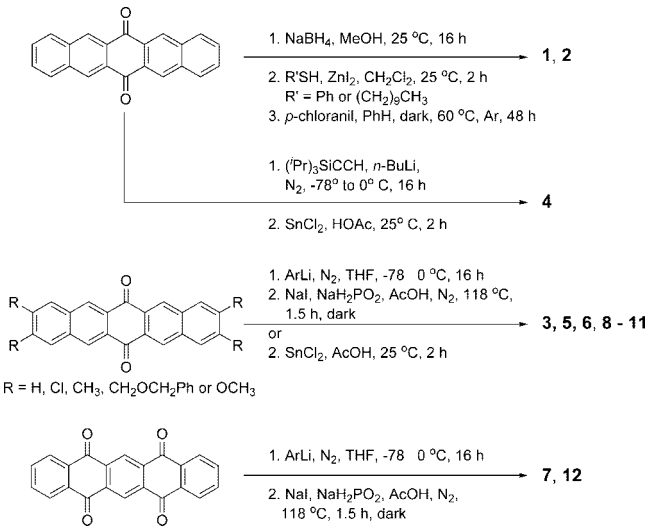

Although limited stages of several reactions appear to follow first-order kinetics, the reactions are not first-order processes. In a first-order reaction, the associated half-life, $t_{1/2}$, would be independent of pentacene derivative concentration and this is not observed in any case. Moreover, plots of ln (A_t/A_o) versus time (A_t is the absorbance at a given wavelength at time t; A_0 is the initial absorbance at the same wavelength at time zero) are not linear over significant percentage conversions for most of the pentacene derivatives tested. These results are in direct conflict with the first-order kinetics reported by Ono and co-workers[2a] for the photooxidation of 6,13-diphenylpentacene, **9**, under similar conditions. These authors reported a first-order rate constant but revealed no absorbance−time data and no details concerning the kinetic analysis. Maliakal and co-workers compared the photooxidation of TIPS-pentacene to that of pentacene in THF solution.[12] They reported that TIPS-pentacene is approximately 50 times more stable than pentacene on the basis of measured half-lives. However, if the photooxidations

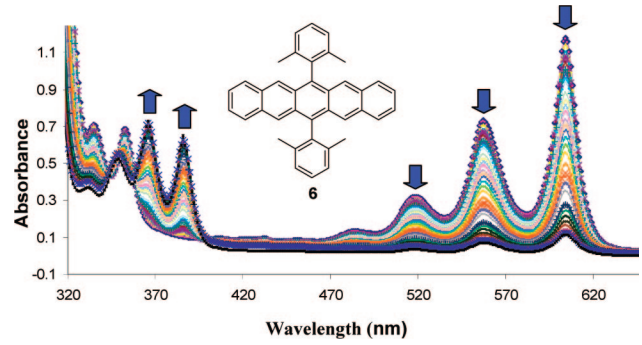

Figure 2. UV−vis spectra associated with the photooxidation of **6**.

Scheme 2. Proposed $^1O_2$ Oxidation of **7** and **12** To Give Diels−Alder Adducts **13** and **14**

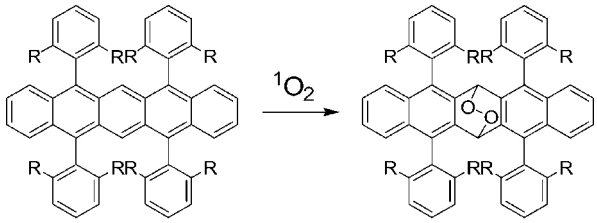

7 R = CH_3 **13** R = CH_3
12 R = H **14** R = H

Scheme 3. Proposed Mechanism for the Oxidation of 6,13-Bis(phenylthio)pentacene **1** and 6,13-Bis(decylthio)pentacene **2** To Afford Pentacene-6,13-dione and the Corresponding Disulfides

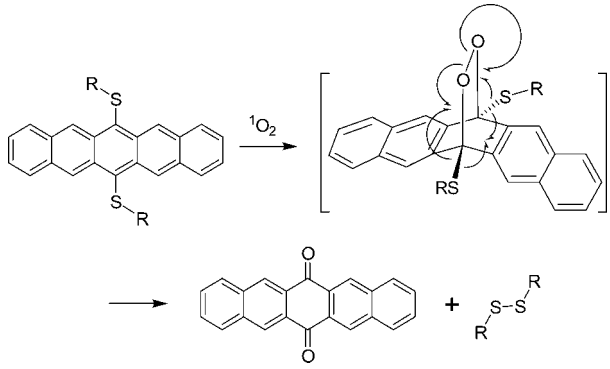

are not first order, then the measured half-lives will vary with initial concentration. Initial concentrations were not provided, but it should be noted that TIPS-pentacene is vastly more soluble than pentacene in THF. In our reactions, pentacene derivatives **1**−**12** were treated to identical conditions such that the measured half-lives could be directly compared. This approach allows for the first time a quantitative assessment of the photooxidative resistances of a large series of pentacene derivatives as a function of substituents.

Pentacene itself could not be quantitatively compared to compounds **1**−**12** as it shows very poor solubility in CH_2Cl_2. For qualitative comparison only, pentacene was saturated in *o*-dichlorobenzene to give a 1.67×10^{-7} M concentration, far lower than the 2.0×10^{-4} M concentrations that were otherwise used. The half-life of "dilute" pentacene in *o*-dichlorobenzene under otherwise identical photooxidative conditions was 7.5 min.

Steric Effects Associated with Phenyl Substituents. The least persistent of the pentacene derivatives tested are the phenyl-substituted derivatives **5**−**12**. Within this series, it is clear that steric resistance is an important contributor to overall persistence. Thus, 6,13-bis(2′,6′-dimethylphenyl)pentacene, **6**, and 5,7,12,14-tetrakis(2′,6′-dimethylphenyl)pentacene, **7**, are more resistant to photooxidation than their counterparts that are missing *o*-methyl groups, 6,13-diphenylpentacene, **9**, and 5,7,12,14-tetraphenylpentacene, **12**, respectively. The low-energy conformations for **6** and **7** place their phenyl rings in near orthogonal orientations relative to the pentacene backbone, and this in turn constrains the *o*-methyl groups of **6** and **7** to lie directly over and under the pentacene π-system, effectively shielding π electrons (Figure 4).

The positional location of phenyl substituents along the acene backbone is important. Thus, **6** is less prone to photooxidation than **7** despite the fact that it has fewer phenyl substituents. The greater persistence of **6** reflects the fact that its *o*-dimethylphenyl substituents provide greater shielding to the most reactive ring on pentacene, i.e., the center ring.[18] Specifically, the 6,13 carbons of the pentacene skeleton, sites for potential Diels−Alder reactions with $^1O_2$, are better shielded in **6** than in **7** (Figure 4). Likewise, **9** is more persistent than **12** for the same reason. Combining steric resistance and positional considerations, it is not surprising that 6,13-bis(2′,6′-diethylphenyl)pentacene, **5**, is considerably more persistent than **6** and that the ordering of longevities for phenyl and *o*-alkylphenyl-substituted pentacenes is as follows: **5** > **6** > **7** > **9** > **12**.

While *o*-alkylphenyl substituents significantly impact pentacene longevity, they have little influence on HOMO−LUMO gaps. Thus, the ortho alkyl substituents on **5** and **6** (λ_{max} = 604−5 nm, $E_{g,optical}$ = 1.95−1.96 eV) do not lead to significant changes in UV−vis spectra and optical HOMO−LUMO gaps as compared to **9** (λ_{max} = 604 nm, $E_{g,optical}$ = 1.94 eV) which lacks ortho alkyl substitution. We also computed HOMO−LUMO gaps for **6** and **9** at the B3LYP/6-311+G**//PM3 level and found minimal differences ($E_{g,DFT}$/eV: **9** (2.23); **6** (2.22), Table 1). Conversely, steric resistance does impact electrochemical HOMO−LUMO gaps as progressively more hindered molecules in the series **9** → **6** → **5** become progressively more difficult to both oxidize and reduce ($E_{g,EChem}$/eV: **9** (1.92); **6** (2.01); **5** (2.04), see Table 1). Rather than indicating a fundamental change in HOMO−LUMO gaps, the electrochemical results reflect the greater degree of difficulty in bringing sterically congested π-systems close to an electrode surface. We conclude that electrochemical HOMO−LUMO gaps can be misleading for pentacene derivatives bearing large substituents. Likewise, **7** and **12** have similar optical HOMO−LUMO gaps (1.90 and 1.88 eV, respectively) but substantially different electrochemical HOMO−LUMO gaps (2.02 and 1.88 eV, respectively).

Electronic Effects Associated with Phenyl Substituents. Phenyl-substituted pentacenes like **3**, **5**, **6**, and **9**−**11** are only partially conjugated because a coplanar conformation between the phenyl rings and the pentacene skeleton is energetically unfavorable. Additional ortho alkyl substitution as in **5** and **6** (λ_{max} = 604−5 nm) does not lead to significant changes in their UV−vis spectra as compared to **9** (λ_{max} = 604 nm), suggesting that the unsubstituted phenyl groups in **9** are already significantly rotated with respect to the pentacene π-system (Table 1). Additional phenyl groups do, however, lead to red-shifted absorptions and smaller optical HOMO−LUMO gaps as in **7** and **12** due to overall enhanced π-delocalization.

Electronic Effects Associated with ED and EW Substituents. An examination of measured half-lives (Figure 1, Table 1) for compounds **3** and **8**−**11** reveals that the inclusion of electron-withdrawing (EW) groups at the 2,3,9,10 positions (i.e., pro-*cata*[19] positions) leads to longer-lived species while the inclusion of electron-donating (ED) groups at the 2,3,9,10 positions has just the opposite effect. Interestingly, the magnitude of these effects is far smaller for ED groups than for EW groups. For example, the half-lives of 2,3,9,10-tetra[(phenylmethoxy)methyl]-6,13-diphenylpentacene, **8**, 2,3,9,10-tetram-

(18) (a) Chien, S.-H.; Cheng, M.-F.; Lau, K.-C.; Li, W.-K. *J. Phys. Chem A* **2005**, *109*, 7509–7518. (b) Cheng, M.-F.; Li, W.-K. *Chem. Phys. Lett.* **2003**, *368*, 630–638. (c) Schleyer, P. v. R.; Manoharan, M.; Jiao, H.; Stahl, F. *Org. Lett.* **2001**, *3*, 3643–3646.

(19) Anthony, J. E.; Gierschner, J.; Landis, C. A.; Parkin, S. R.; Sherman, J. B.; Bakus, R. C. *Chem Commun.* **2007**, 4746–4748. (a) See also: Medina, B. M.; Anthony, J. E.; Gierschner, J. *ChemPhysChem* **2008**, *9*, 1519–1523.

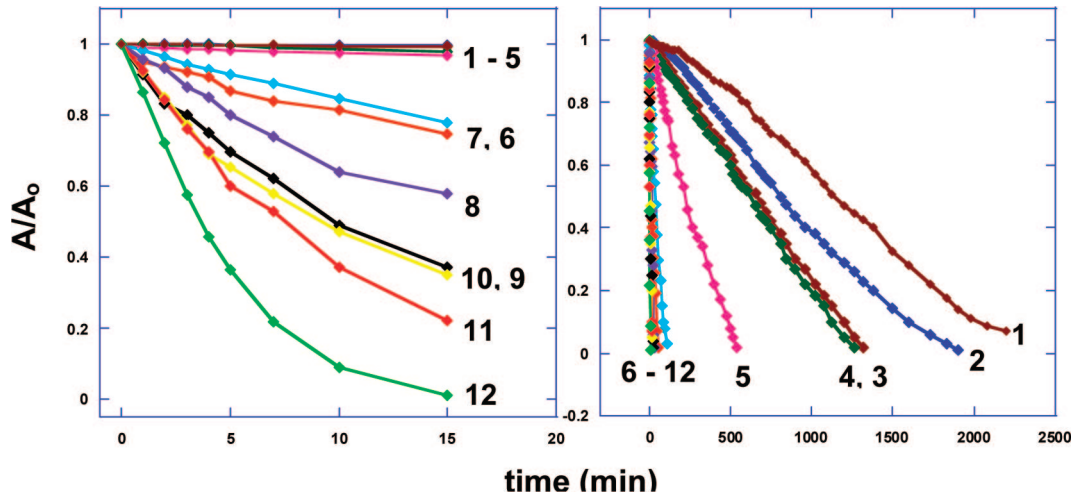

Figure 3. Absorbance−time profiles for pentacene derivatives **1**−**12**.

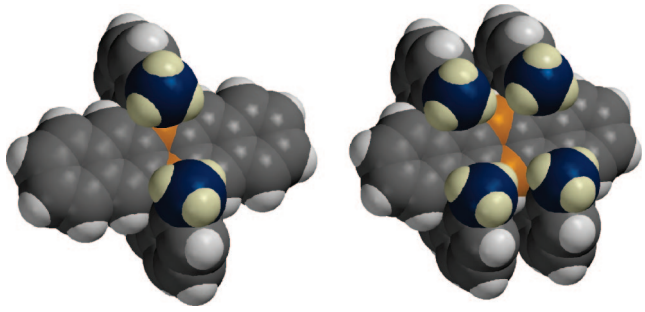

Figure 4. MM2 calculated structures for 6,13-bis(2′,6′-dimethylphenyl)-pentacene, **6** (left), and 5,7,12,14- tetrakis(2′,6′-dimethylphenyl)pentacene, **7** (right). For clarity, methyl carbons are shown in blue, methyl hydrogens in beige, and the reactive 6,13 carbons of the pentacene skeleton in orange.

ethyl-6,13-diphenylpentacene, **10**, and 2,3,9,10-tetramethoxy-6,13-diphenylpentacene, **11**, are only modestly different from that of **9** which lacks 2,3,9,10 substituents. Thus, pentacene **11** with pro-*cata* methoxy groups (Hammett $\sigma_p = -0.27$[20]) is marginally less persistent than **10** with pro-*cata* methyl groups (Hammett $\sigma_p = -0.17$[20]) which is in turn marginally less persistent than **8** with pro-*cata* (phenylmethoxy)methyl groups (Hammett $\sigma_p \approx +0.08$[20,21]). In the case of **8**, the additional steric resistance provided by the large (phenylmethoxy)methyl groups may also enhance its longevity but only to a small extent as these groups are well removed from the reactive, center ring. Conversely, the EW chlorine substituents (Hammett $\sigma_p = +0.23$[20]) on 2,3,9,10-tetrachloro-6,13-bis(2′,6′-dimethylphenyl-)pentacene, **3**, effectively increase its half-life by more than an order of magnitude compared to **6**. With a combination of EW chlorine substituents and sterically demanding 2′,6′-dimethylphenyl substituents, **3** is in fact more persistent than TIPS-pentacene, **4**, widely regarded as one of the most stable pentacene derivatives.[5b]

Interestingly, a comparison of λ_{max} values and optical HOMO−LUMO gaps ($E_{g,optical}$) for **3** and **6** (Table 1) reveals only small differences. Electrochemically determined frontier orbital energies provide an explanation. Thus, 2,3,9,10 halogen substitution reduces both the HOMO and LUMO energies of **3** to nearly equal extents. The small reduction in HOMO−LUMO gap observed for **3** is due to a slightly larger depression of its LUMO energy level. A review of the anthracene literature is consistent with this finding and reveals that the magnitude of substituent effects on UV−vis spectra and optical HOMO−LUMO gaps is very strongly dependent upon the positional locations of the substituents,[22] as illustrated in Figure 5. Here, we see that chlorine, fluorine, and phenyl substituents all lead to red-shifted anthracene derivatives with smaller optical HOMO−LUMO gaps. Remarkably, however, two chlorine atoms attached to the center ring at the 9,10 positions have a substantially larger impact on the optical HOMO−LUMO gap than do eight fluorine atoms in the 1,2,3,4,5,6,7,8 positions. We conclude that the center rings of acenes are not only the most reactive but also the most sensitive to substituent HOMO−LUMO gap effects.

It was previously noted[19] that oxygen atoms bound directly to the pro-*cata* positions as in **11** cause a significant blue-shift of the low-energy UV−vis absorptions (e.g., $\Delta\lambda_{max} = 18-21$ nm for the three lowest-energy absorption bands of **11** as compared to those of **9**, see Table 1). With relatively small basis set DFT calculations as a guide, this unusual electronic effect was explained[19] as a special inductive stabilization of the HOMO, leading to an overall larger HOMO−LUMO gap. We find this argument to be flawed (*vide infra*). Compared to **9**, pentacene derivatives **8**, **10**, and **11** are increasingly easier to oxidize, indicating greater electron donation into the corresponding pentacene π-systems upon moving from (phenylmethoxy)methyl (**8**: Hammett $\sigma_p \approx +0.08$[20,21] $\Delta E_{1/2}$ [O] (**9**−**8**) = 55 mV) to methyl (**10**: Hammett $\sigma_p = -0.17$,[20] $\Delta E_{1/2}$ [O] (**9**− **10**) = 146 mV) to methoxy (**11**: Hammett $\sigma_p = -0.27$,[20] $\Delta E_{1/2}$ [O] (**9**−**11**) = 218 mV) substituents. Likewise, derivative **11** with pro-*cata* O substitution possesses the highest energy HOMO in the series (HOMO (eV): **9**: −5.00; **8**: −4.93; **10**: −4.86; **11**: −4.78). At the same time, derivatives **8**, **10** and **11** are increasingly more difficult to reduce as compared to **9** ($\Delta E_{1/2}$ [red] (**9**−**8**) = 34 mV; $\Delta E_{1/2}$ [red] (**9**−**10**) = 125 mV; $\Delta E_{1/2}$ [red] (**9**−**11**) = 255 mV) indicating progressively higher energy LUMOs (LUMO (eV): **9**: −3.08; **8**: −3.07; **10**: −2.97; **11**: −2.84). The electrochemical HOMO−LUMO gaps for **8** ($E_{g,EChem} = 1.86$) and **10** ($E_{g,EChem} = 1.89$) shrink as compared to **9** ($E_{g,EChem} = 1.92$) because their pro-*cata* substituents raise their HOMO energies slightly more than their corresponding

(20) Dean, J. A. *Handbook of Organic Chemistry*; McGraw-Hill: New York, 1987; pp 7.1−7.7.
(21) A σ_p value for the−CH_2−OH is cited in place of−CH_2−O−CH_2Ph.
(22) Tannaci, J. F.; Noji, M.; McBee, J.; Tilley, T. D. *J. Org. Chem.* **2007**, *72*, 5567–5573.

Table 1. Electrochemical and Optical Properties of Pentacene Derivatives **1**− **12**

pentacene derivatives ($t_{1/2}$)	$E_{1/2}$ [O][a](mV)	$E_{1/2}$ [red][a](mV)	E_{HOMO} (eV)[b]	E_{LUMO} (eV)[b]	$E_{g,EChem}$ (eV)[b]	low-energy λ_{max} (nm)	$E_{g,optical}$ (eV)[c]	$E_{HOMO,DFT}$, $E_{LUMO,DFT}$ (eV)[d]	$E_{g,DFT}$ (eV)[d]
1 (1140)	849, 1093	−1099	−5.17	−3.36	1.81	624, 575, 534	1.86	−5.20, −3.03	2.17
2 (750)	755, 936	−1229, −1726	−5.07	−3.26	1.81	617, 570, 529	1.88	−5.08[e], −2.89[e]	2.19[e]
3 (620)	899	−1227	−5.21	−3.24	1.97	605, 559, 520	1.94	−	−
4 (520)	789	−1054	−5.11	−3.42	1.69	643, 591, 548	1.81	−5.08, −3.07	2.01
5 (220)	713	−1485	−5.03	−2.99	2.04	605, 558, 520	1.95	−	−
6 (40)	695	−1478	−5.01	−3.00	2.01	604, 557, 518	1.96	−4.93, −2.71	2.22
7 (13)	638, 1372	−1543	−4.95	−2.93	2.02	618, 569, 529	1.90	−	−
8 (9.0)	627, 1224	−1430	−4.93	−3.07	1.86	600, 554, 515	1.93	−	−
9 (8.5)	682	−1396	−5.00	−3.08	1.92	604, 558, 519	1.94	−4.86, −2.63	2.23
10 (7.3)	536, 1171	−1521	−4.86	−2.97	1.89	602, 556, 518	1.92	−	−
11 (6.6)	464, 1081	−1651	−4.78	−2.84	1.94	583, 539, 501	2.01	−	−
12 (3.7)	635, 1183	−1407	−4.95	−3.07	1.88	621, 573, 532	1.88	−4.80, −2.59	2.21
pentacene (7.5)[f]						582, 537, 501	2.08	−2.67, −4.96	2.29

[a] Recorded $E_{1/2}$ values vs Ag/Ag^+ in CH_2Cl_2 with $TBAPF_6$ as supporting electrolyte. [b] HOMO and LUMO energies and electrochemical HOMO−LUMO gaps determined from the onset of the first oxidation and the first reduction waves in cyclic voltammograms. [c] Optical HOMO−LUMO gaps determined from the onset of lowest-energy visible absorption band. The onset is defined as the intersection between the baseline and a tangent line that touches the point of inflection. [d] Calculations performed at the B3LYP/6-311+G**//PM3 level. [e] Calculation for analogous 6,13-bis-(methylthiophenyl)pentacene rather than **2**. [f] Saturated pentacene in *o*-dichlorobenzene (1.67×10^{-7} M); all other compounds (**1**−**12**) in CH_2Cl_2 at 2.0×10^{-4} M.

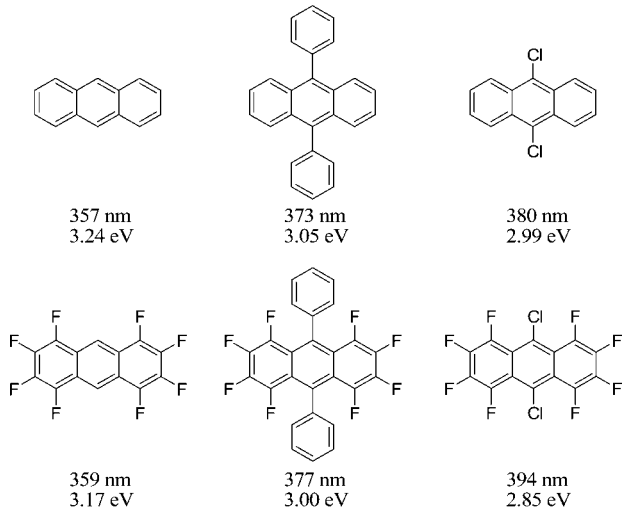

Figure 5. λ_{max} and $E_{g,optical}$ values for anthracene derivatives reported in ref 22.

LUMO energies. For **11**, however, the opposite is observed. The electrochemical HOMO−LUMO gap of **11** ($E_{g,EChem}$ = 1.94) is larger than that of **9** because pro-*cata* O substitution raises LUMO energies slightly more than it raises the corresponding HOMO energies. Thus, the unique electronic effect exhibited by pro-*cata* O substitution (blue shifting, larger HOMO−LUMO gaps) is not due to unusually lowered HOMO energies[19] but rather to disproportionately higher LUMO energies.

Probing Electronic Effects with DFT Calculations. We computed the frontier orbital energies and HOMO−LUMO gaps for pentacene and several derivatives (i.e., **1**, **2**, **4**, **6**, **9**, **12**, see Table 1). The results indicate that B3LYP/6-311+G**//PM3 HOMO−LUMO gaps are systematically 0.3 ± 0.04 eV higher than optical HOMO−LUMO gaps for all molecules tested except pentacene and TIPS-pentacene **4** where they are only 0.2 eV high. Similarly, B3LYP/6-311+G**//PM3 HOMO−LUMO gaps are 0.34 ± 0.04 eV higher than measured electrochemical HOMO−LUMO gaps for all pentacene derivatives tested except **6** where steric resistance leads to an artificially large electrochemical HOMO−LUMO gap (*vide supra*). Interestingly, B3LYP/6-311+G**//PM3 calculations reproduce HOMO energies well but consistently predict higher than expected LUMO energies and this is the root cause of the systematically overstated HOMO−LUMO gaps. Nonetheless, the experimental HOMO, LUMO and associated gap trends are all well represented at the B3LYP/6-311+G**//PM3 level, corroborating the recent demonstration[23] that triple-ζ quality AO basis sets enable more reliable energy calculations.

Electronic Effects Associated with Ethynyl and Silylethynyl Substituents. While it is not the longest lived species, TIPS-pentacene **4** has an unusually long wavelength of absorption (λ_{max} = 643 nm) and an unusually small HOMO−LUMO gap (optical, electrochemical, DFT: see Table 1) compared to all other derivatives synthesized. Based upon double-ζ valence basis set DFT calculations,[12] Maliakal and co-workers concluded that the small HOMO−LUMO gap of TIPS-pentacene is largely attributable to an unusually low LUMO energy. Our electrochemical measurements and B3LYP/6-311+G**//PM3 calculations concur with this finding but provide no special insight that would explain this electronic effect. In fact, despite the widespread use of silylethynyl groups as substituents on acenes, a theoretical explanation for their unique electronic effects has yet to be proposed.

In **4**, the silylethynyl group is fully conjugated to the acene π-system (resonance effect) and the *sp* hybridized ethynyl carbons are modestly more electronegative than the sp^2 hybridized carbons to which they are attached (inductive effect). Are these effects sufficient to account for the unusually low LUMO energy? The answer appears to be yes. As illustrated in Figure 6, we compared frontier orbitals and HOMO−LUMO gaps for the series pentacene, 6,13-diphenylpentacene, 6,13-bis(thiomethyl)pentacene, 6,13-dichloropentacene, 6,13-dicyanopentacene, 6,13-diethynylpentacene and 6,13-bis(trimethylsilylethynyl)pentacene, all calculated at the B3LYP/6-311+G**//PM3 level. Compared to pentacene, all of the derivatives exhibited lower HOMO and LUMO energies and at least a modest reduction in the associated gap. However, those derivatives with *sp* hybridized carbons attached directly to the pentacene skeleton experience a disproportionate lowering of their LUMO energies such that their corresponding HOMO−LUMO gaps are substantially smaller. The presence of a trialkylsilyl group as in 6,13-bis(trimethylsilylethynyl)pentacene or TIPS-pentacene appears

(23) Grimme, S.; Steinmetz, M.; Korth, M. *J. Org. Chem.* **2007**, *72*, 2118–2126.

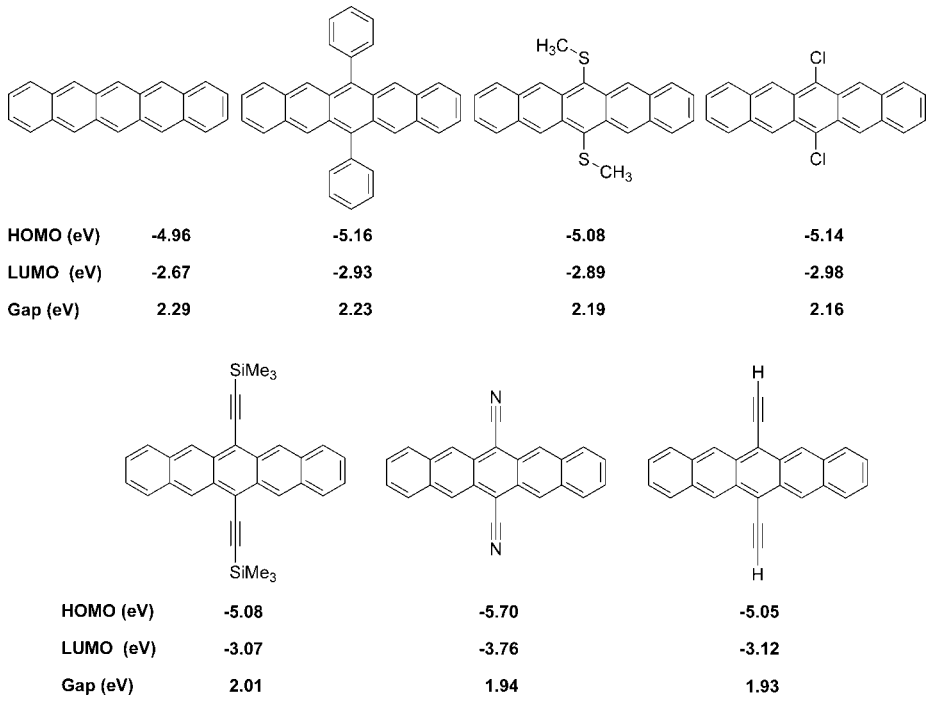

Figure 6. HOMO and LUMO energies and associated HOMO−LUMO gaps for pentacene, 6,13-diphenylpentacene, 6,13-bis(thiomethyl)pentacene, 6,13-dichloropentacene, 6,13-bis(trimethylsilylethynyl)pentacene, 6,13-dicyanopentacene and 6,13-diethynylpentacene. All energies were calculated at the B3LYP/6-311+G** level, the first five following a PM3 optimization and the last two following a B3LYP/6-311+G** optimization.

to be of little significance where HOMO and LUMO energies and associated gaps are concerned. Indeed, 6,13-diethynylpentacene possesses a similar HOMO energy, a lower LUMO energy and an overall reduced gap as compared to 6,13-bis(trimethylsilylethynyl)pentacene. Most impressive, however, is 6,13-dicyanopentacene which exhibits a spectacularly low LUMO energy and an overall smaller HOMO−LUMO gap than 6,13-bis(trimethylsilylethynyl)pentacene (and TIPS-pentacene). Based on these results, we predict that 6,13-dicyanopentacene will be exceptionally easy to reduce and quite amenable for use as an n-type organic semiconductor.[24]

Alkylthio and Arylthio Substituents. Of all the pentacene derivatives tested, the most persistent are 6,13-bis(phenylthio)-pentacene, **1**, and 6,13-bis(decylthio)pentacene, **2** (Figure 1, Table 1). Both are considerably longer-lived than TIPS-pentacene **4** and both are soluble in a variety of organic solvents. As such, they represent promising, new candidates for thin-film OFET, OLED[15] and organic photovoltaic[16] (OPV) devices. Steric resistance cannot account for the enhanced longevity of **1** and **2** as compared to other pentacene derivatives tested. The phenylthio and decylthio groups of **1** and **2** are not constrained to lie over their respective pentacene π-systems, as are for example the *ortho*-methyl groups of **6** and **7** (Figure 4), and are not expected to provide unusual shielding. Electronically, alkylthio and arylthio groups could be impacting the pentacene π-system through either inductive effects or resonance effects or both. The UV−vis spectra for **1** and **2** reveal red-shifted absorptions at 624 and 617 nm, respectively, among the longest wavelength bands observed in the series **1**−**12** (Table 1). Only TIPS-pentacene **4**, 5,7,12,14-tetrakis(*o*-methylphenyl)pentacene, **7**, and 5,7,12,14-tetraphenylpentacene **12** show similar absorption bands with λ_{max} values greater than 615 nm. Likewise, these five compounds possess the smallest optical HOMO−LUMO gaps in the series **1**−**12** (Table 1). As illustrated in Figure 5, red-shifted UV−vis bands and reduced HOMO−LUMO gaps result from both EW (inductive effect) and conjugated (resonance effect) substituents at the center-most ring of an acene and it is therefore difficult to pinpoint the nature of alkylthio and arylthio electronic effects based upon optical data. Electrochemically, **1** and **2** are among the most difficult derivatives to oxidize (Figure 7) and possess relatively low HOMO energies, comparable to **4** but surpassed by **3** which bears EW chlorine substituents in the 2,3,9,10 positions. This result suggests a relatively strong inductive effect for alkylthio and arylthio substituents. Consistent with this conclusion, **1** and **2** are also amongst the easiest derivatives to reduce (Figure 7). They possess relatively low LUMO energies, comparable to **3** but falling short of **4** in this regard. These redox features distinguish **1** and **2** from phenyl-substituted pentacene derivatives where resonance effects and steric resistance are believed to dominate. But is a strong inductive effect involving S sufficient to explain the dramatically enhanced photooxidative resistances of **1** and **2**? The answer must be no as **1** and **2** are not electronically remarkable compared to the shorter lived species **3** and **4**. A sulfur specific substituent effect may be at play for **1** and **2**. We have considered that alkylthio and arylthio substituents may enable physical (as opposed to chemical) quenching of $^1O_2$. Physical quenching of this type would effectively protect the pentacene π-system from a $^1O_2$ type II photooxidation (*vide infra*). Indeed, several sulfide species are known to physically quench $^1O_2$[25] via formation of a weak complex which returns $^1O_2$ to $^3O_2$ through one of several processes including radia-

(24) The highly interesting synthetic target 6,13-dicyanopentacene has yet to be synthesized. It and other cyanated pentacene derivatives have been studied computationally with an emphasis on calculated internal reorganization energies. See: Kuo, M.-Y.; Chen, H.-Y.; Chao, I. *Chem.−Eur. J.* **2007**, *13*, 4750–4758.

(25) (a) Bonesi, S. M.; Fagnoni, M.; Monti, S.; Albini, A. *Tetrahedron* **2006**, *62*, 10716–10723. (b) Bonesi, S. M.; Fagnoni, M.; Monti, S.; Albini, A. *Photochem. Photobiol. Sci.* **2004**, *3*, 489–493.

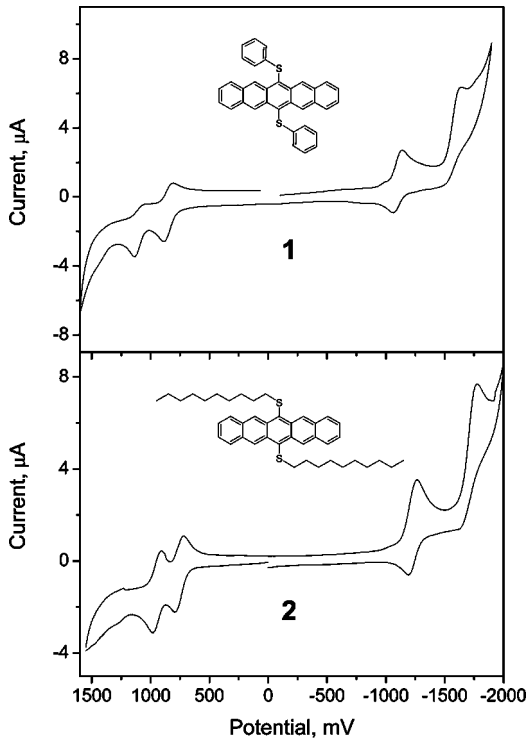

Figure 7. Cyclic voltammograms for **1** and **2** recorded in CH_2Cl_2 at room temperature using a freshly cleaned Pt working electrode and $TBAPF_6$ as supporting electrolyte.

Scheme 4. Type II Photooxidation Pathways for Acenes: $^1O_2$ Sensitization (a) and Electron Transfer (b)

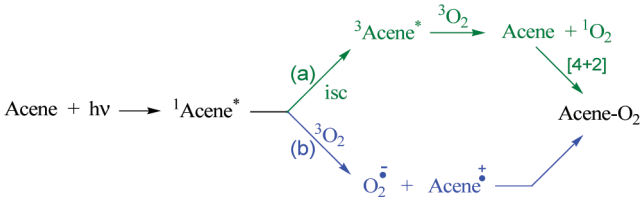

tionless paths.[26] Physical quenching of $^1O_2$ is often highly competitive with chemical quenching, especially when nonpolar, aprotic solvents are utilized as they were in this study.[25] In order to probe possible physical quenching of $^1O_2$ by select substituents, competition experiments involving the reactions between several pentacene derivatives and thermally generated $^1O_2$ are planned.

Mechanism of Degradation. Photoexcited pentacenes are believed to sensitize $^1O_2$ formation,[2,12] and numerous examples of acene−$^1O_2$ Diels−Alder adducts are known[2a,27] in addition to those reported here (Schemes 2 and 3). The clean formation of acene−$^1O_2$ Diels−Alder adducts suggests a type-II photooxidation mechanism[28] as in path (a) of Scheme 4. It is however possible to achieve the same products via an alternative type-II mechanism involving electron transfer[28] (ET) from photoexcited pentacene to $^3O_2$ followed by O−C couplings, as in path (b) of

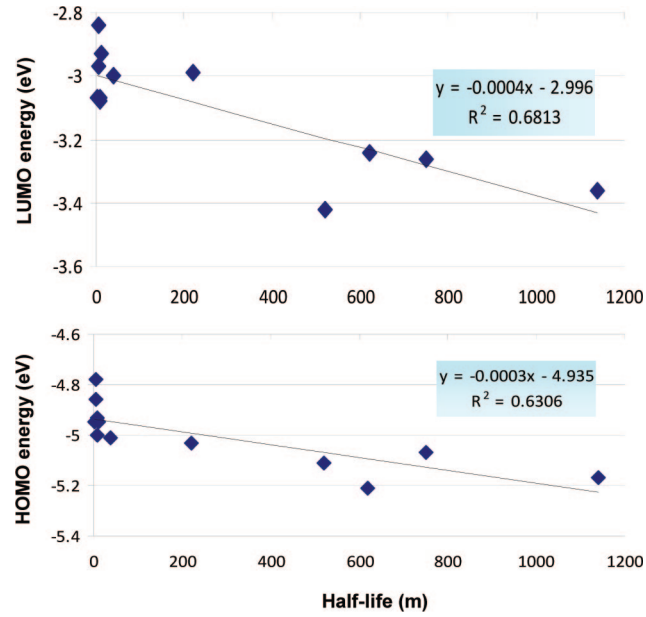

Figure 8. HOMO and LUMO energies for **1**−**12** plotted as a function of measured half-life.

Scheme 4. Indeed, several of the substituent effects revealed here could be simultaneously argued as evidence for either a $^1O_2$ or an ET type-II path. For example, the enhanced photooxidative resistance accompanying 2,3,9,10-tetrachloro substitution could be explained as an inductive effect which either renders **3** less dienophilic toward $^1O_2$ (i.e., reduced HOMO energy) or less prone to undergo a photoexcited electron transfer with triplet oxygen, $^3O_2$ (i.e., reduced LUMO energy).

Malikal and co-workers argued that $^1O_2$ sensitization (path (a), Scheme 4) can be ignored for TIPS-pentacene **4** because their calculated singlet−triplet energy gap for **4** is well below the 22.5 kcal/mol singlet−triplet energy gap for $^1O_2$.[12] They further argued that the lower LUMO energy of **4** compared to that of pentacene results in enhanced photostabilization as the barrier to electron transfer (path (b), Scheme 4) is proportionately greater. We find these arguments unconvincing for two reasons: (1) the calculations[12] were performed with a relatively small double-ζ valence basis set (B3-LYP/6-31+G*) which is known to give unreliable energies;[23] (2) conclusions are based upon a comparison of only two molecules. Regarding the first point, it is documented that B3-LYP DFT calculations are well suited for predicting geometries at the 6-31G* level. However, it has also been shown[23] that triple-ζ quality AO basis sets represent a minimum requirement for reliable energy calculations and that the 6-31G* basis set should be avoided in accurate work. Regarding the second point, our data demonstrate that compounds **1**−**3** possess higher LUMO energies than **4** and are nonetheless more persistent under photooxidative conditions.

In order to evaluate potential type-II photooxidation mechanisms for compounds **1**-**12**, we looked for correlations between measured half-lives and frontier orbital energies. If a $^1O_2$ type-II photooxidation mechanism with rate determining Diels−Alder cycloaddition is dominant for compounds **1**-**12**, then one should see a correlation between measured half-lives and pentacene HOMO energies. Conversely, if an ET type-II photooxidation mechanism with rate determining ET is dominant, then one should see a correlation between measured half-lives and pentacene LUMO energies.[12] Figure 8 reveals that both HOMO and LUMO energies trend with measured half-lives but neither

(26) Schweitzer, C.; Schmidt, R. *Chem. Rev.* **2003**, *103*, 1685–1757.
(27) (a) Kaur, I.; Miller, G. P. *New J. Chem.* **2008**, *32*, 459–463. (b) Yamada, H.; Yamashita, Y.; Kikuchi, M.; Watanabe, H.; Okujima, T.; Uno, H.; Ogawa, T.; Ohara, K.; Ono, N. *Chem. Eur. J.* **2005**, *11*, 6212–6220. (c) Gollnick, K. *Adv. Chem. Ser.* **1968**, 78–101. (d) Zhou, X.; Kitamura, M.; Shen, B.; Nakajima, K.; Takahashi, T. *Chem. Lett.* **2004**, *33*, 410–411.
(28) Foote, C. S. *Photochem. Photobiol.* **1991**, *54*, 659.

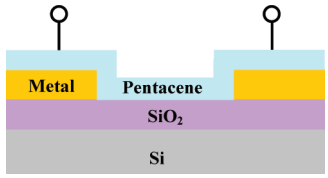

Figure 9. Device for current−voltage measurements.

provides a satisfactory fit. It is possible that the identified reaction steps are not rate-determining, that the actual mechanism involves a combination of type II pathways, that the dominant pathway changes as a function of substituent, or that the photooxidation mechanism is not described in Scheme 4. A recent theoretical paper predicts, for example, a stepwise biradical path for $^1O_2$ addition to pentacene.[29] Photodimerization could also be contributing to degradation of some pentacene derivatives. It is known to be significant for pentacene[11b] and TIPS-pentacene[11a] in the absence of O_2. Further work is required in order to fully elucidate the mechanism(s) of degradation.

Current−Voltage Characterization of Thin-Film Pentacene Derivatives. Thin-film devices prepared using highly soluble pentacene derivatives should be amenable to large area, high rate, low-cost manufacturing methods such as spin casting, printing technologies, and reel-to-reel processing with flexible substrates. Solution-based thin-film formation typically requires additional processing steps above and beyond casting. These include evaporation of solvent (usually at elevated temperatures) and thermal annealing to produce high-quality films. In a low-cost manufacturing environment, these heat treatment steps would occur in air. Thus, it is important that soluble pentacene derivatives exhibit significant solution and thin-film stability in air at elevated temperatures. Of the 12 pentacene derivatives synthesized here, only TIPS-pentacene **4** has been subjected to thin-film electronic characterization.[5] Four of the compounds studied, **1**−**3** and **5**, also warrant testing in thin-film electronic devices due to their photooxidative resistances and their excellent solubilities in a variety of organic solvents. We studied the surface morphology of solution-processed thin-films of **2** and **5** and made preliminary current−voltage (I−V) measurements on the device schematically illustrated in Figure 9. Thus, a 500 nm thick SiO_2 insulating layer was thermally grown on 3 in. Si wafers. Chromium/gold (50 Å/700 Å) metal electrodes were patterned using standard optical lithography. The distance between the two metal electrodes was 5 μm. Prior to deposition, the wafers were treated with hexamethyldisilazane.[30] Dichloromethane solutions of **2** and **5** were spin coated onto the wafers at 1500 rpm for one minute. The coated wafers were then thermally annealed for 1 min at 60 °C followed by 90 s at 200 °C in order to reduce the density of grain boundaries.[31] Following heat treatment, the morphologies of the pentacene films were inspected using an optical microscope and a scanning electron microscope (SEM). The images (Figure 10) provide details about the thin-film characteristics of **2** and **5** after thermal annealing. Spin coated thin-films of **5** are ordered with grain sizes of 150−300 nm (Figure 10 b,c), suitable for device fabrication. Continuous conduction paths through the film are observed between the electrodes. Grains produced by spin coating **2** were well distributed (Figure 10 d,e) but larger in size, less continuous and overall less desirable for device fabrication (Figure 10 e,f). In the future, alternative processing options will be explored including drip and blade coating. Variables such as choice of solvent, temperature and time of evaporation, and temperature and time of thermal annealing will be examined.

The I−V measurements were performed in ambient air at room temperature (23 °C) in the dark, as illustrated in Figure 11. They indicate that the device prepared from **5** with a large number of continuous conduction paths between electrodes has a much higher conductance than the device prepared from **2**. For example, at a 20 V positive bias, the current measured for the thin-film **5** device is much higher (~225 μA) than that measured for the thin-film **2** device (~131 nA). Both devices show a relatively low onset voltage of approximately 5V, similar to the I−V behavior reported by Ruppel and co-workers for a defect-free thin-film pentacene diode.[32]

Summary, Conclusions, and Future Direction

A combined experimental and computational study for a large series of pentacene derivatives including six newly synthesized compounds has revealed several key findings: (1) the photooxidative resistances of substituted pentacenes are impacted by both steric and electronic factors; (2) sterically demanding substituents such as *o*-alkyl phenyl groups maximally enhance photooxidative resistance when they are located at the 6,13 positions of the center ring rather than the penultimate rings; (3) substituent HOMO−LUMO gap effects are largest when the substituents are located at the 6,13 positions of the center ring; (4) the addition of electron withdrawing chlorines to the 2,3,9,10 positions (i.e., pro-*cata* positions) leads to substantially longer-lived species while the addition of electron donating groups to the same positions leads to marginally shorter-lived species; (5) a combination of 2,3,9,10-tetrachloro and 6,13-*o*-alkyl phenyl substituents yields a pentacene derivative, **3**, that is more resistant to photooxidation than TIPS-pentacene; (6) the unique electronic effect exhibited by 2,3,9,10 oxygen substitution (blue-shifting, larger HOMO−LUMO gap) is not due to unusually lowered HOMO energies as previously reported but rather to disproportionately higher LUMO energies; (7) EW groups such as halogens, ethynyl, silylethynyl, alkylthio, and arylthio groups located at the 6,13 positions reduce HOMO−LUMO gaps by lowering LUMO energies more than they lower HOMO energies; (8) derivatives with ethynyl substituents at the 6,13 position experience a disproportionate lowering of their LUMO energies such that their corresponding HOMO−LUMO gaps are substantially smaller; (9) experimental HOMO, LUMO, and associated gap trends are all well represented at the B3LYP/6-311+G**//PM3 level; (10) B3LYP/6-311+G**//PM3 calculations indicate that 6,13-dicyanopentacene is a particularly attractive synthetic target that will possess a very low LUMO energy and a significantly smaller HOMO−LUMO gap than TIPS-pentacene; (11) 6,13-bis(phenylthio)pentacene, **1**, and 6,13-bis(decylthio)pentacene, **2**, are substantially longer-lived than TIPS-pentacene under photooxidation conditions; (12) derivatives **1** and **2** possess relatively small HOMO−LUMO gaps, show excellent solubility in a variety of organic solvents

(29) Reddy, A. R.; Bendikov, M. *Chem. Commun.* **2006**, 1179–1181.
(30) (a) Voorthuyzen, J. A.; Keskin, K.; Bergveld, P. *Surf. Sci.* **1987**, *187*, 201–211. (b) Hosoi, Y.; Tsunami, D.; Ishii, H.; Furukawa, Y. *Chem. Phys. Lett.* **2007**, *436*, 139–143. (c) Moggia, F.; Videlot-Ackermann, C.; Ackermann, J.; Raynal, P.; Brisset, H.; Fages, F. *J. Mater. Chem.* **2006**, *16*, 2380–2386.
(31) Kang, S. J.; Noh, M.; Park, D. S.; Kim, H. J.; Whang, C. N. *J. Appl. Phys.* **2004**, *95*, 2293–2296.
(32) Ruppel, L.; Birkner, A.; Witte, G.; Busse, C.; Lindner, T.; Paasch, G.; Wöll, C. *J. Appl. Phys.* **2007**, *102*, 033708.

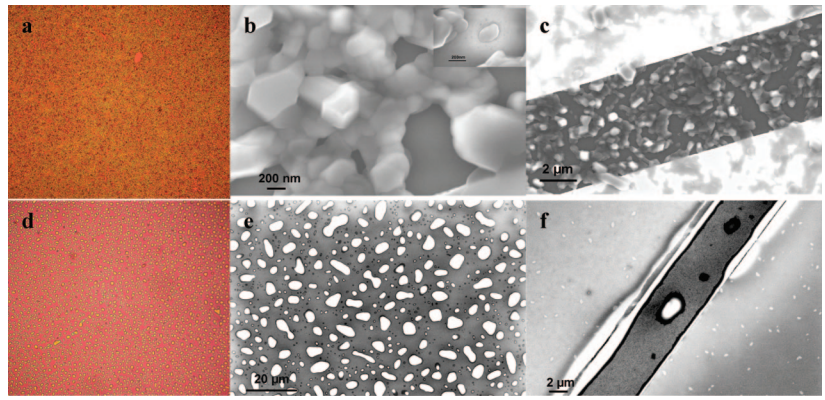

Figure 10. Optical and Scanning Electron Microscope images of solution-processed thin-films of **5** (a-c) and **2** (d-f). (a) Optical image of thin-film **5** taken at 50X magnification after thermal annealing; (b) SEM image after thermal annealing revealing a relatively uniform and continuous thin-film of **5**; (c) SEM image of thin-film of **5** between electrodes; (d) optical image of **2** taken at 50X magnification after thermal annealing; (e) SEM image after thermal annealing of irregularly shaped microstructures of **2** forming a discontinuous film; (f) SEM image of a sample area of lowest coverage obtained from devices made with **2**.

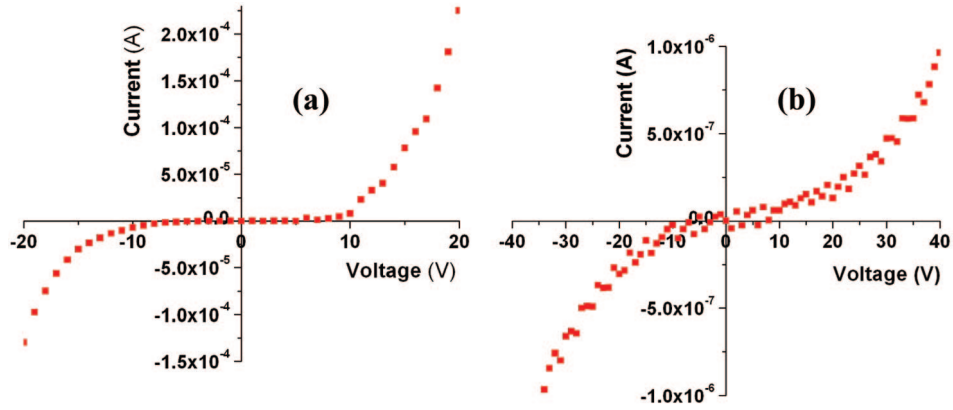

Figure 11. Measured I−V curves from thin-film devices made from **5** (a) and **2** (b). The device prepared from **5** has a large number of continuous conduction paths between electrodes and a conductance at 20 V that is approximately 3 orders of magnitude greater than that prepared from **2**.

and seem ideally suited for thin-film electronic device applications provided high quality thin-films with continuous conduction paths can be prepared.

Lessons learned studying substituent effects in pentacene derivatives are applicable to larger acenes (e.g., hexacene, heptacene, octacene, nonacene, etc.) which are highly interesting species from both a fundamental chemistry perspective as well as a potential device applications perspective. They are, however, almost completely unexplored due to their poor solubility and low resistance to photooxidation. Future work will include the synthesis of large acenes bearing alkylthio and arylthio substituents. If persistent and amenable to high-quality thin-film formation, these compounds may find immediate application in organic electronic devices due to their predicted lower reorganization energies, reduced HOMO−LUMO gaps, and higher charge carrier mobilities.[5b]

Experimental Section

General Remarks. 2-Bromo-*m*-xylene, 2-bromo-1,3-diethylbenzene, phenyllithium (1.8 M solution in di-*n*-butyl ether), and *n*-butyllithium (2.5 M solution in hexanes) were purchased from Aldrich. Thiophenol, 1-decanethiol, 4,5-dichlorobenzene-1,2-dicarboxylic acid, and triisopropylsilyl acetylene were purchased from TCI America. All purchased reactants and reagents were used without further purification. All reactions, unless otherwise noted, were carried out under the protection of N_2. All reaction containers were flame dried under vacuum before use. Solvents were purified by standard methods and dried if necessary. ^{1}H NMR (500 MHz) spectra were recorded with a Varian AC 500 spectrometer. ^{1}H and ^{13}C NMR samples were internally referenced to TMS (0.00 ppm). Mass spectra were determined on LDI-TOF-MS (Shimadzu-Biotech) mass spectrometer.

High-resolution mass spectra were recorded at the Notre Dame mass spectrometry facility.

UV−Vis Spectroscopy and Kinetic Studies. UV−visible spectra were obtained on a Nikolet Evolution 300 spectrometer using 1 cm quartz cells. Dilute solutions (2.0×10^{-4} M) of pentacene derivatives were prepared using degassed spectroscopic grade dichloromethane. The cells were protected from light until each experiment began, at which point an initial spectrum was recorded. Each cell was then exposed to air by loosening the cap to allow for free exchange of air, while minimizing solvent evaporation. The cells were placed on a laboratory bench under conventional 32 W, SP35 fluorescent lighting (General Electric, 2850 lm). The solutions were repeatedly scanned at prescribed intervals until less than 5% of the starting acene remained.

Cyclic Voltammetry. Cyclic votammetry (CV) studies of each pentacene derivative were performed using a BAS-100B electrochemical analyzer in a three-electrode single-compartment cell with a Pt working electrode, Ag/AgCl reference electrode, and a Pt wire as auxiliary electrode. Tetrabutylammonium

hexafluorophosphate, $TBAPF_6$, was used as supporting electrolyte (0.1 M), and HPLC grade dichloromethane was used as solvent (no further purification). A scan rate of 100 mV/s was typically employed. The concentration of pentacene derivative was typically 0.5 mM. The Pt working electrode required cleaning between samples, especially before and after characterization of S containing **1** and **2**. HOMO and LUMO energies and electrochemical HOMO−LUMO gaps were determined from the onsets of the first oxidation and the first reduction waves.

6,13-Bis(phenylthio)pentacene (1). Compound **1** was prepared according to the procedure of Kobayashi and co-workers.[14] Thus, pentacene-6,13-dione was converted to *trans*-6,13-dihydroxy-6,13-dihydropentacene in 91% yield. Chloranil dehydrogenation of *trans*-6,13-phenylthio-6,13-dihydropentacene yielded **1** in 71% yield. HRMS (FAB) m/z = 494.1172, calcd m/z = 494.1163 (Error = +1.9 ppm).

6,13-Bis(*n*-decylthio)pentacene (2). Compound **2** was prepared according a modified Kobayashi procedure.[14] Thus, to a mixture of *trans*-6,13-dihydroxy-6,13-dihydropentacene (1.0 g, 3.20 mmol) and ZnI_2 (1.02 g, 3.20 mmol) were added dry CH_2Cl_2 (100 mL) and 1-decanethiol (1.23 g, 7.03 mmol) at RT under an Ar atmosphere. The resulting mixture was stirred at RT for 2 h and then quenched with H_2O. The mixture was extracted with CH_2Cl_2, and the organic layer was washed with brine and dried over anhydrous Na_2SO_4. After evaporation of solvents, the residue was purified by silica gel column chromatography using *n*-hexanes/CH_2Cl_2 (2:1) as eluant to give *trans*-6,13-bis(*n*-decylthio)-6,13-dihydropentacene as a colorless viscous oil (1.80 g, 90% yield). ^{1}H NMR (500 MHz, $CDCl_3$): δ 7.86 (m, 4H), 7.74 (s, 4H), 7.51 (m, 4H), 5.24 (s, 2H), 2.67 (t, 4H, J = 7.40 Hz), 1.69 (m, 4H), 1.42 (m, 4H), 1.30 (m, 24H), 0.93 (t, 6H, J = 6.63 Hz). ^{13}C NMR (125.68 MHz, $CDCl_3$): δ 135.3, 132.6, 127.7, 127.4, 126.2, 48.0, 33.9, 32.0, 29.7, 29.7, 29.5, 29.4, 22.3, 29.3, 22.8, 14.3. LDI-MS m/z: 624 [M^+], 451 [$M^+ - S(CH_2)_9CH_3$], 278 [$M^+ - 2(S(CH_2)_9CH_3)$]. A mixture of *trans*-6,13-bis(*n*-decylthio)-6,13-dihydropentacene (1.10 g, 1.76 mmol), chloranil (0.87 g, 3.52 mmol), and K_2CO_3 (2.43 g, 17.6 mmol) was stirred in dry benzene (170 mL) at 60 °C for 48 h under an Ar atmosphere in the dark. After cooling to RT, the reaction mixture was filtered and washed with CH_2Cl_2. Following evaporation of the filtrate, the solid residue was triturated with *n*-hexanes, filtered, and washed with hexane. The filtrate was evaporated again, and the solid residue was passed through a short column of *n*-Al_2O_3 using CH_2Cl_2 as eluant. The deep blue band was collected and the solvent evaporated to give pure **2** as a deep blue solid (0.81 g, 74% yield). ^{1}H NMR (500 MHz, $CDCl_3$): δ 9.71 (s, 4H), 8.05 (m, 4H), 7.40 (m, 4H), 3.03 (t, 4H, J = 7.07 Hz), 1.55 (m, 4H), 1.41 (m, 4H), 1.25 (m, 4H), 1.16 (m, 20H), 0.86 (t, 6H, J = 7.07 Hz). ^{13}C NMR (125.68 MHz, $CDCl_3$): δ 132.9, 132.8, 132.1, 128.9, 127.0, 126.0, 38.2, 32.0, 30.2, 29.7, 29.6, 29.4, 29.3, 29.0, 22.8, 14.2. LDI-MS m/z: 622 [M^+], 481 [$M^+ - (CH_2)_9CH_3$], 340 [$M^+ - 2((CH_2)_9CH_3)$], UV−vis λ_{max} (nm): 617, 570, 529. HRMS (FAB) m/z = 622.3666, calcd m/z = 622.3667 (Error = −0.2 ppm).

2,3,9,10-Tetrachloro-6,13-bis(2′,6′-dimethylphenyl)pentacene (3). Initially, 4,5-dichlorobenzene-1,2-dicarbaldehyde was prepared as described by Farooq.[33] The dialdehyde was converted to 2,3,9,10-tetrachloropentacene-6,13-dione (70% yield, LDI-MS m/z: 446 [M^+]) according to Wudl.[34] A solution of 1-bromo-2,6-dimethylbenzene (0.59 g, 3.19 mmol) was stirred in dry THF (30 mL) and cooled to −78 °C in a dry ice/acetone bath. *n*-Butyllithium (2.5 M, 1.08 mL, 2.7 mmol) was added, and the solution was stirred for 5 h at −78 °C. The 2,3,9,10-tetrachloropentacene-6,13-dione (0.2 g, 0.45 mmol) was then added to the pale yellow solution, and the mixture was allowed to gradually warm to RT with stirring (14 h). To the reaction mixture was added 1 M HCl (50 mL). Following extraction with CH_2Cl_2 (100 mL), the organic layer was washed with water and dried over $CaCl_2$. The solvent was removed under vacuum until only ~10 mL remained, at which point hexanes (100 mL) were added, resulting in the formation of a white precipitate. The 2,3,9,10-tetrachloro-6,13-bis(2′,6′-dimethylphenyl)-6,13-dihydropentacene-6,13-diol was isolated by vacuum filtration (0.22 g, 74%, LDI-MS m/z: 656 [M^+], 639 [$M^+ - OH$], 622 [$M^+ - 2(OH)$]) and used without further purification. A suspension of 2,3,9,10-tetrachloro-6,13-bis(2′,6′-dimethylphenyl)-6,13-dihydropentacene-6,13-diol (0.13 g, 0.20 mmol), NaI_2 (0.2 g, 1.33 mmol), and sodium hypophosphite monohydrate (0.22 g, 2.07 mmol) in glacial acetic acid (10 mL) was boiled for 1.5 h under N_2 in a round-bottom flask equipped with a reflux condenser and wrapped in foil to block ambient light. After cooling, the reaction mixture was filtered and washed with water (40 mL) and methanol (25 mL). After drying at reduced pressure, **3** was obtained in 81% yield (0.1 g). ^{1}H NMR (500 MHz, $CDCl_3$): δ 8.05 (s, 4H), 7.90 (s, 4H), 7.50 (t, 2H, J = 7.56 Hz), 7.39 (d, 4H, J = 7.56 Hz), 1.78 (s, 12H). ^{13}C NMR (125.68 MHz, $CDCl_3$): δ 138.0, 137.5, 130.2, 130.0, 129.2, 128.6, 128.5, 128.1, 125.6, 124.6, 22.9. LDI-MS m/z: 626.5[M^+], 624.5[M^+], 622.5[M^+], 589 [$M^+ - Cl$], 554 [$M^+ - 2Cl$], UV−vis λ_{max} (nm): 605, 559, 520. HRMS: very weak molecular ions observed at m/z 622−628 with appropriate pattern for tetrachloro substitution; stronger ($M^+ - Cl + H$) signal observed: (FAB) m/z = 588.1157, calcd m/z = 588.1178 (Error = −3.6 ppm).

6,13-Bis(triisopropylsilylethynyl)pentacene (4). TIPS-pentacene **4** was prepared using the Swager modification[17] of Anthony's synthesis.[9] HRMS (FAB) m/z = 638.3767, calcd m/z = 638.3764 (Error = +0.5 ppm).

6,13-Bis(2′,6′-diethylphenyl)pentacene (5). Compound **5** was prepared as previously described.[27a] HRMS (FAB) m/z = 542.2971, calcd m/z = 542.2973 (Error = −0.5 ppm).

6,13-Bis(2′,6′-dimethylphenyl)pentacene (6). Compound **6** was prepared as previously described.[7a] HRMS (FAB) m/z = 486.2341, calcd m/z = 486.2348 (Error = −1.4 ppm).

5,7,12,14-Tetrakis(2′,6′-dimethylphenyl)pentacene (7). A procedure analogous to that described above for **3** was utilized for the synthesis of **7**. Thus, 2-bromo-1,3-dimethylbenzene (4.34 g, 23.45 mmol), *n*-BuLi (2.5 M, 7.84 mL, 19.6 mmol), and pentacene-5,7,12,14-tetraone (0.4 g, 1.18 mmol) were reacted as above to yield as mixture of 5,7,12,14- tetrakis(2′,6′-dimethylphenyl)pentacene-5,7,12,14-tetrahydro-5,7,12,14-tetrol isomers in 63% crude yield (0.57 g, MS-LDI m/z: 762 [M^+], 745 [$M^+ - OH$], 728 [$M^+ - 2(OH)$], 711 [$M^+ - 3(OH)$], 694 [$M^+ - 4(OH)$]). The mixture of 5,7,12,14-tetrakis(2′,6′-dimethylphenyl)pentacene-5,7,12,14-tetrahydro-5,7,12,14-tetrol isomers (0.4 g, 0.53 mmol) was reacted with sodium iodide (1.09 g, 7.27 mmol) and sodium hypophosphite monohydrate (1.2 g, 11.32 mmol) to afford **7** (0.34 g, 93%). ^{1}H NMR (500 MHz, $CDCl_3$): δ 7.67 (s, 2H), 7.44 (m, 4H), 7.21 (t, 4H, J = 7.56 Hz), 7.13 (m, 4H), 7.09 (d, 8H, J = 7.56

(33) Farooq, O. *Synthesis* **1994**, 1035–1036.

(34) Perepichka, D. F.; Bendikov, M.; Meng, H.; Wudl, F. *J. Am. Chem. Soc.* **2003**, *125*, 10190–10191.

Hz), 1.7 (s, 24H). ^{13}C NMR (125.68 MHz, $CDCl_3$): δ 137.6, 137.5, 135.6, 129.0, 128.5, 127.5, 127.2, 126.8, 125.0, 123.7, 20.0. MS-LDI *m/z*: 694 [M^+]. UV−vis λ_{max} (nm): 618, 569, 529. HRMS (FAB) *m/z* = 694.3575, calcd *m/z* = 694.3599 (Error = −3.6 ppm).

2,3,9,10-Tetra[(phenylmethoxy)methyl)]-6,13-diphenylpentacene (8). To a dry 500 mL three-neck flask equipped with a thermometer and a dropping funnel was added a solution of dry CH_2Cl_2 (75 mL) and oxalyl chloride (3.35 mL, 35.23 mmol) under Ar. The stirred solution was cooled to −78 °C, and a solution of DMSO (5 mL, 0.07 mol) in CH_2Cl_2 (13 mL) was added dropwise. This solution was stirred for 5 min before a solution of 4,5-bis[(phenylmethoxy)methyl]benzene-1,2-dimethanol[35] (4.55 g, 12.03 mmol) in CH_2Cl_2/DMSO (25 mL) was added dropwise. The reaction was allowed to continue for 0.5 h, and then triethylamine (40 mL, 0.28 mol) was slowly added at −78 °C. The reaction mixture was stirred for 10 min and then allowed to warm slowly to RT. Ice-cold water (50 mL) was added to the reaction mixture, and the aqueous layer was extracted with CH_2Cl_2 (2 × 50 mL) and then dried over $CaCl_2$. Evaporation of solvent gave crude 4,5-bis[(phenylmethoxy)methyl]benzene-1,2-dicarbaldehyde which was further purified by silica gel column chromatography using hexane/ethyl acetate (70:30) as eluant to yield pure 4,5-bis[(phenylmethoxy)methyl]benzene-1,2-dicarbaldehyde in 70% yield (3.15 g). ^{1}H NMR (500 MHz, $CDCl_3$): δ 10.54 (s, 2H), 8.08 (s, 2H), 7.35 (m, 10H), 4.65 (s, 4H), 4.59 (s, 4H). ^{13}C NMR (125.68 MHz, $CDCl_3$): δ 192.3, 142.6, 137.5, 135.6, 130.9, 128.7, 128.1, 128.0, 73.2, 68.7. 4,5-Bis[(phenylmethoxy)methyl]benzene-1,2-dicarbaldehyde (1.35 g, 3.61 mmol) and 1,4-cyclohexanedione (0.21 g, 1.88 mmol) were stirred in 60 mL of ethanol. To this was added 10 mL of 5% KOH dropwise with stirring. Upon addition of the first drop, the solution darkened, and solids began to precipitate. The reaction mixture was stirred at RT for 1 h and then boiled for 2 h. After cooling to RT, the solids were filtered, washed with water, and then dried to give yellow-brown 2,3,9,10-tetrakis-[(phenylmethoxy)methyl]pentacene-6,13-dione (0.68 g, 46%). ^{1}H NMR (500 MHz, $CDCl_3$): δ 8.92 (s, 4H), 8.17 (s, 4H), 7.39 (m, 16H), 7.35 (m, 4H), 4.80 (s, 8H), 4.64 (s, 8H). ^{13}C NMR (125.68 MHz, $CDCl_3$): δ 183.1, 138.6, 138.0, 134.9, 131.0, 129.6, 129.5, 128.7, 128.1, 128.1, 73.0, 69.9. LDI-MS *m/z*: 789 [M^+]. A solution of 2,3,9,10-tetrakis-[(phenylmethoxy)methyl]pentacene-6,13-dione (0.2 g, 0.25 mmol) was stirred under N_2 and cooled to −78 °C in a dry ice/acetone bath. Upon cooling, phenyllithium (1.8 M, 5.41 mL, 9.74 mmol) was added dropwise over 10 min. The resulting dark green solution was allowed to warm to RT and then stirred for 14 h. The reaction mixture was quenched with 1 M HCl (50 mL) and the resulting orange brown solution was extracted with CH_2Cl_2 (100 mL), washed with water, and then dried over $CaCl_2$. The solvent was evaporated until only ∼10 mL remained, at which point hexanes (100 mL) were added, resulting in the formation of a brown precipitate, crude 2,3,9,10-tetrakis-[(phenylmethoxy)methyl]-6,13-diphenyl-6,13-dihydropentacene-6,13-diol. The diol was isolated by vacuum filtration (0.23 g, 95%). The crude diol was not subjected to further purification. ^{1}H NMR (500 MHz, $CDCl_3$): δ 8.29 (s, 4H), 7.76 (s, 4H), 7.72 (m, 4H), 7.68 (m, 2H), 7.63 (m, 4H), 7.34 (m, 16H), 7.30 (s, 4H) 4.71 (s, 8H), 4.56 (s, 8H). ^{13}C NMR (125.68 MHz, $CDCl_3$): δ 139.7, 138.3, 137.2, 134.0, 131.9, 130.5, 129.0, 128.8, 128.6, 128.5, 128.0, 127.9, 127.8, 125.6, 72.6, 70.7. LDI-MS *m/z*: 944 [M^+], 927 [M^+ − OH], 911 [M^+ − 2(OH)]. To a solution of crude 2,3,9,10-tetrakis-[(phenylmethoxy)methyl]-6,13-diphenyl-6,13-dihydropentacene-6,13-diol (0.24 g, 0.25 mmol) in acetone (10 mL) was added dropwise a solution of $SnCl_2$ (0.34 g, 1.79 mmol) in 50% glacial acetic acid (5 mL). The mixture was stirred at RT for 2 h. The blue precipitate was filtered, and the solids were washed with water and dried to afford pure 2,3,9,10-tetra[(phenylmethoxy)methyl)]-6,13-diphenylpentacene, **8**, in 82% yield (0.19 g). ^{1}H NMR (500 MHz, $CDCl_3$): δ 8.29 (s, 4H), 7.76 (s, 4H), 7.72 (m, 4H), 7.68 (m, 2H), 7.63 (m, 4H), 7.34 (m, 16H), 7.30 (s, 4H) 4.71 (s, 8H), 4.56 (s, 8H). ^{13}C NMR (125.68 MHz, $CDCl_3$): δ 139.7, 138.3, 137.2, 134.0, 131.9, 130.5, 129.0, 128.8, 128.6, 128.5, 128.0, 127.9, 127.8, 125.6, 72.6, 70.7. LDI-MS *m/z*: 911 [M^+], UV−vis λ_{max} (nm): 600, 554, 515. HRMS (FAB) *m/z* = 910.4010, calcd *m/z* = 910.4022 (Error = −1.3 ppm).

6,13-Diphenylpentacene (9). 6,13-Diphenyl-6,13-dihydropentacene-6,13-diol was prepared as previously described[36] in 72% yield. ^{1}H NMR (500 MHz, $CDCl_3$): δ 8.44 (s, 4H), 7.96 (m, 4H), 7.56 (m, 4H), 6.88 (t, 2H, *J* = 7.20 Hz), 6.79 (m, 8H). ^{13}C NMR (125.68 MHz, $CDCl_3$): δ 142.6, 139.6, 132.8, 128.3, 127.8, 127.5, 127.1, 126.5, 125.4, 76.5. LDI-MS *m/z*: 464 [M^+], 447 [M^+-OH], 430 [M^+-2(OH)]. A suspension of 6,13-diphenyl-6,13-dihydropentacene-6,13-diol (0.5 g, 1.08 mmol), NaI (1.10 g, 7.34 mmol) and sodium hypophosphite monohydrate (1.21 g, 11.42 mmol) in glacial acetic acid (25 mL) was boiled for 1.5 h under N_2 in a round-bottom flask that was equipped with a reflux condenser. The flask was wrapped in foil to block ambient light. After cooling, the reaction mixture was filtered and washed with water (50 mL) and methanol (25 mL). After drying at reduced pressure, compound **9** was obtained in 88% yield (0.41 g). ^{1}H NMR (500 MHz, C_6D_6): δ 8.60 (s, 4H), 7.58 (m, 4H), 7.45 (m, 4H), 7.40 (m, 2H), 7.36 (m, 4H), 6.89 (m, 4H). ^{13}C NMR (125.68 MHz, $CDCl_3$): δ 139.8, 137.1, 131.9, 131.1, 128.8, 128.7, 128.7, 127.9, 125.7, 125.3. LDI-MS *m/z*: 430 [M^+], UV−vis λ_{max} (nm): 604, 558, 519. HRMS (FAB) *m/z* = 430.1703, calcd *m/z* = 430.1722 (Error = −4.4 ppm).

2,3,9,10-Tetramethyl-6,13-diphenylpentacene (10). Initially, 4,5-dimethylbenzene-1,2-dicarbaldehyde was prepared as described by Farooq.[33] 4,5-Dimethylbenzene-1,2-dicarbaldehyde (1.0 g, 6.17 mmol) and 1,4-cyclohexanedione (0.38 g, 3.39 mmol) were stirred in 60 mL of ethanol. To this was added 10 mL of 5% KOH dropwise with stirring. Upon addition of the first drop, the solution darkened, and solids began to precipitate. The reaction mixture was stirred at RT for 1 h and then boiled for 2 h. After cooling to RT, the solids were filtered, washed with water, and dried to give crude, brown 2,3,9,10-tetramethylpentacene-6,13-dione (1.00 g, 81%). LDI-MS *m/z*: 364 [M^+]. 2,3,9,10-Tetramethylpentacene-6,13-dione (0.5 g, 1.37 mmol) was reacted with a solution of phenyllithium (1.8 M, 4.57 mL, 8.23 mmol) as described above to give crude 2,3,9,10-tetramethyl-6,13-diphenyl-6,13-dihydropentacene-6,13-diol (0.54 g, 75%, LDI-MS *m/z*: 520 [M^+], 503 [M^+ − OH], 486 [M^+ − 2(OH)]). The diol (0.5 g, 0.96 mmol) was reacted with NaI (1.00 g, 6.67 mmol) and sodium hypophosphite monohydrate (1.10 g, 10.38 mmol) to furnish **10** (0.43 g, 91%). ^{1}H NMR (500 MHz, $CDCl_3$): δ 8.14 (s, 4H), 7.70 (m, 4H), 7.65 (m, 2H), 7.62 (m, 4H), 7.48 (s, 4H), 2.35 (s, 12H). ^{13}C NMR (125.68 MHz, $CDCl_3$): δ 140.2, 136.3, 135.5, 132.0, 130.7, 128.7, 128.5, 127.6,

(35) Meissner, R.; Garcias, X.; Mecozzi, S.; Rebek, J., Jr. *J. Am. Chem. Soc.* **1997**, *119*, 77–85.

(36) (a) Allen, C. F. H.; Bell, A. *J. Am. Chem. Soc.* **1942**, *64*, 1253. (b) Maulding, D. R.; Roberts, B. G. *J. Org. Chem.* **1969**, *34*, 1734.

127.1, 123.8, 20.5. LDI-MS *m/z*: 486 [M^+], UV−vis λ_{max} (nm): 602, 556, 518. HRMS (FAB) *m/z* = 486.2320, calcd *m/z* = 486.2348 (Error = −5.7 ppm).

2,3,9,10-Tetramethoxy-6,13-diphenylpentacene (11). 1,2-Bis-(bromomethyl)-4,5-dimethoxybenzene was prepared as described.[37] 1,2-Bis(bromomethyl)-4,5-dimethoxybenzene (2.27 g, 7.00 mmol), benzoquinone (0.38 g, 3.50 mmol, and NaI (5.36 g, 35.7 mmol) were dissolved in dry DMF (100 mL) and stirred in a sealed vessel at 110 °C for two days. The reaction mixture was cooled to room temperature, and the solids were filtered. The solids were washed with water and acetone and then dried in air overnight to yield crude, yellow 2,3,9,10-tetramethoxypentacene-6,13-dione (0.90 g) in 60% yield. ^{1}H NMR (500 MHz, $CDCl_3$): δ 8.73 (s, 4H), 7.35 (s, 4H), 4.08 (s, 6H). LDI-MS *m/z*: 428 [M^+]. Using a procedure analogous to that described above, 2,3,9,10-tetramethoxypentacene-6,13-dione (0.5 g, 1.17 mmol) was reacted with a solution of phenyllithium in di-*n*-butylether (1.8 M, 4.20 mL, 7.57 mmol) to afford 2,3,9,10-tetramethoxy-6,13-diphenyl-6,13-dihydropentacene-6,13-diol (0.49 g, 72%). The diol (0.5 g, 0.86 mmol) was then treated with $SnCl_2$ (1.44 g, 7.57 mmol) in 50% glacial acetic acid (5 mL). The mixture was stirred at RT for 2 h. The blue precipitate was filtered, and the solids were washed with water and dried to afford pure **11** (0.43 g, 91%). ^{1}H NMR (500 MHz, $CDCl_3$): δ 8.04 (s, 4H), 7.73 (m, 4H), 7.68 (m, 2H), 7.64 (m, 4H), 6.92 (s, 4H) 3.95 (s, 6H). ^{13}C NMR (125.68 MHz, $CDCl_3$): δ 150.3, 140.4, 135.1, 132.1, 128.8, 128.4, 127.9, 127.5, 122.6, 104.5, 56.0. LDI-MS *m/z*: 550 [M^+], UV−vis λ_{max} (nm): 583, 539, 501. HRMS (FAB) *m/z* = 551.2226, calcd *m/z* = 551.2222 (Error = +0.7 ppm).

5,7,12,14-Tetraphenylpentacene (12). Compound **12** was prepared as previously described.[38] HRMS (FAB) *m/z* = 582.2354, calcd *m/z* = 582.2348 (Error = +1.0 ppm).

6,13-Epidioxy-6,13-dihydro-5,7,12,14-tetrakis(2′,6′-dimethylphenyl)pentacene (13). A solution of **7** (10 mg) in CH_2Cl_2 (10 mL) was exposed to air for 2 h at RT. Compound **13** was isolated by evaporating solvent. ^{1}H NMR (500 MHz, $(CD_3)_2CO$): δ 7.48 (m, 4H), 7.40 (m, 4H), 7.24 (t, 4H), 7.18 (d, 4H, *J* = 7.56 Hz), 7.12 (d, 4H, *J* = 7.56 Hz), 5.39 (s, 2H), 1.93 (s, 12H), 1.81 (s, 12H). ^{13}C NMR (125.68 MHz, $(CD_3)_2CO$): δ 138.7, 138.2, 136.7, 134.9, 133.8, 133.4, 129.9, 129.4, 129.1, 128.7, 128.1, 76.8, 22.4, 21.4. LDI-MS *m/z*: 726 [M^+], 710 [M^+ − (O)], 694 [M^+ − 2(O)].

6,13-Epidioxy-6,13-dihydro-5,7,12,14-tetraphenylpentacene (14). [2c,39] A solution of **12** (10 mg) in CH_2Cl_2 (10 mL) was exposed to air for 2 h at RT. Compound **14** was isolated by evaporating solvent. ^{1}H NMR (500 MHz, $CDCl_3$): δ 7.65 (m, 4H), 7.40 (m, 12H), 7.36 (m, 4H), 7.31 (m, 4H), 7.13 (d, 4H, *J* = 7.56 Hz), 6.21 (s, 2H). ^{13}C NMR (125.68 MHz, $CDCl_3$): δ 136.1, 135.0, 132.2, 132.1, 130.8, 130.7, 128.7, 128.5, 127.7, 127.2, 126.5, 75.3. LDI-MS *m/z*: 614 [M^+], 598 [M^+ − (O)], 582 [M^+ − 2(O)].

Acknowledgment. We acknowledge the National Science Foundation (Nanoscale Science & Engineering Center for High-rate Nanomanufacturing, NSF-0425826) and Nantero, Inc. for financial support of this work. We also acknowledge Professor William Heineman of the University of Cincinnati for helpful discussions concerning the electrochemistry of pentacene derivatives.

Supporting Information Available: ^{1}H and ^{13}C NMR spectra, LDI mass spectra, UV−vis spectra, absorbance−time profiles, cyclic voltammograms, key intermediates, oxidation products. This material is available free of charge via the Internet at http://pubs.acs.org.

JA804515Y

(37) Diederich, F.; Jonas, U.; Gramlich, V.; Herrmann, A.; Ringsdorf, H.; Thilgen, C. *Helv. Chim. Acta* **1993**, *76*, 2445–2453.

(38) (a) Miller, G. P.; Briggs, J. *Proc. Electrochem. Soc.* **2002**, 2002–2012. (b) *Fullerenes: The Exciting World of Nanocages and Nanotubes*; Kamat, P. V., Guldi, D. M., Kadish, K. M., Eds.; The Electrochemical Soc.: Pennington, NJ, 2002; Vol. 12, pp 279−284.

(39) Sparfel, D.; Gobert, F.; Rigaudy, J. *Tetrahedron* **1980**, *36*, 2225–2235.